Design and Modeling Optimization of Superheated Micro Steam Power Plant

[1]Daramola S. F., [1,2]Kareem B., and [3]Oladosu K. O

[1]Department of Mechanical Engineering, Federal University of Technology, Akure, Nigeria

[2]Department of Mechanical and Mechatronics Engineering, Achievers University Owo, Nigeria

[3]Department of Mechanical Engineering, Kwara State University, Molete, Nigeria

DOI: https://doi.org/10.51584/IJRIAS.2025.101100137

Received: 09 December 2025; Accepted: 16 December 2025; Published: 26 December 2025

ABSTRACT

A PKS-fired 5-10 kW micro power plant has been designed, modeled and simulated to produce superheated steam for domestic and SMEs consumption. The target is to sustain power output at optimal design parameters. Design, modeling and simulation analyses of plant's components were carried and then integrated to a unit micro power plant. These analyses were done to enhance the efficiency of whole power plant through reduction of heat losses and optimal sizing of components. Modeling results indicated that running the plants at the lowest possible temperatures (pressures) of 235 ^{o}C (0.35 MPa) and 235 ^{o}C (0.35 MPa) would be sufficient to enhance safety with acceptable steam mass flow rates (0.00357 kg/s, 0.00178) and steam flow velocities (14.87 m/s, 7.43 m/s). Design results showed that angular mild steel of diameter ranging 5 -10 mm were adequate for the plant stand. Simulation results revealed that the designed parameters (stress, strain, deflection, and thermal resistance) were within the acceptable standards, this portrayed design adequacy. Designed temperature of 0- 400^{o}C was within the acceptable range and far from maximum tolerable material temperature of 1200^{o}C. Heat flux (2.31 W/mm^{2}) obtained from the design was conveniently within the simulated range, which shows that the design is workable. Improvement efficiency of 12% was obtained as compared to past micro plant design; this is a remarkable achievement.

Keywords: Micro steam plant, PKS, Optimal design parameters, Safety, Efficiency

INTRODUCTION

The pre-requisite for socio-economic development of an area includes the provision of basic infrastructure such as good roads, water, electricity and other social amenities (Ekpo, 2005). Energy is central and life blood of engineering activities globally (Ekpo, 2012; Makoju, 2003). There is a great demand for electricity energy, which is in short supply (Ozoro, 2003). It was revealed that the electricity per capital consumption has a strong correlation with National GDP, and that only about 10% of rural households have access to electricity (Makoju, 2003). These challenges have been looked into in the past (Awosope and Okoye, 2003). As part of solution efforts, this study develops a scalable micro steam generator that utilizes biomass (Palm Kernnel Shell, Husk, etc.) as fuel to generate steam for industrial application. Biomass is a renewable energy source which may also include biodegradable wastes that can be used as fuel (Ajayi, 2007). In industry, biomass can be used to generate electricity with steam turbines in place (Oladosu, 2016). Biomass wastes when left to decay may lead to environmental nuisance (Binstocks, 1989). The main energy recovery goal for the palm oil industry is to provide steam and electricity for the mill operations (Mohammed et al., 2011). This can also be extended for household and commercial usage or by direct connection to the national grid. Utilizing waste from oil palm for energy purposes could help prevent global warning resulting from emission of CO_2 and other green house gases (Mohammed et al., 2014)

A sustainable source of power supply through the use of biomass as fuel in furnace to generate superheated steam will in no measure play a significant role towards providing power for domestic and SMEs applications.

The existing micro steam generators (Astrom and Bell 2000; Yin et al., 2008; Oladosu, 2016) are deficient of inability to regulate: the water supply into the boiler section and the release of steam from the boiling chamber to the turbine; and heat distribution at the heating chamber for effective heating. Redesign of the steam generator to include: mechanical regulators for water, fuel (biomass) and steam), location of steam drum inside the boiler compartment, and heat lost reduction lagging-mechanism using bi-refractory bricks/fibre glass).

In this study a scalable PKS-fired micro power plant for superheated steam production is designed towards provision of a scalable superheated steam power for domestic and SMEs consumption. The technology featured improvement on the past micro power plant designs (Oladosu, 2016) for enhanced performance efficiency. This operational designed is limited to 5-10 kW capacity. Thermodynamic operations of the micro power plant fired by the Palm Kernel Shell (PKS) were not fully covered in the design.

LITERATURE REVIEW

Grate-fired boilers can fire a wide range of fuels of varying moisture contents and show great potential in biomass combustion (Marrow, 2005). According to jekayinfa and Bamgbose (2008), Joller et al. (2007), about 0.07 tons of palm shell, 0.103 tons of palm fibre and 0.012 tons of kernel are produced as the solid wastes. Paper and pulp that are obtained by processing the oil palm wastes can be used in so many ways such as cigarette paper and bond paper for writing (MNNA, 2001). Palm kernel shell (PKS) has been proposed for use as concrete reinforcement in construction industry (Najmi et al., 2007; Okpula et al., 1990). PKS has been used as admixture with Portland cement for production concrete (Oladosu et al 2016). PKS has been mixed with activated carbon for industrial use (Adewumi and Ogedengbe, 2005). In addition oil palm trunks mixed with EFB has been combusted to produce electrical energy (Sumanttin and Chai, 2008). The use of palm shells and palm fibres for the production of briquettes has also been reported by Hussain et al. (2002). In all these studies, it is evident that PKS has higher calorific value.

Fixed bed combustion is appropriate for biomass fuel with high moisture content, varying particle sizes and high ash content. A good and well controlled grate is designed to guarantee a homogenous distribution of the fuel and the bed of residue over the whole grate surface. In addition, a staged combustion should be obtained by separating the primary and secondary combustion chamber in order to avoid back mixing of the secondary air and to separate gasification and oxidation zone (Sjaak and Jaap, 2008). The better the mixing quality between flue gas and secondary combustion air, the lower the amount of excess oxygen required for complete combustion in the power plant (Oladosu, 2016).

Fluidized bed boilers have recently been used in steam generator. In fluidized bed boilers, biomass and the additives are suspended in a combustion chamber by air blowing up through the bed. The amount of fluidization that occurs depends on the size of the fuel and velocity of the air moving through the bed (Sjaak and Jaap, 2008). In palm oil processing industry, biomass residues can be converted from being potential environmental pollutants to useful fuel for steam and electricity generation which are largely needed for industrial use (Pelfersson and Steenar, 2009). Nigeria, being the fifth largest producer of palm oil in the world accounts for about 1.5% (930,000 metric tons) of the global output (Izah et al., 2016). However, a huge quantity of oil palm residues which could otherwise be used for energy generation is being wasted. These oil palm residues if utilized can generate a great percentage of electricity (Mohammed et al., 2014). This can significantly reduce green house gases emissions and increase employment for local population (Khullar, 1995).

Fixed bed grate combustor has been applied in this study due to its simplicity of design and enhancement of combustion with less oxygen requirement due to better mixing quality between flue gas and secondary combustion air.

It is necessary to have a comprehensive understanding of fuel characteristics during the designing of combustion equipment and boiler plant (Aho, 2001). The lower moisture and ash contents of the PKS fuel make it a good choice in firing technology (Adeline, 2012). Grate firing system and fluidized bed combustor are technologies suitable for reducing ash rich fuels. This challenge has been tackled previously (Oladosu, 2016). This study focused only on utilization of heat content of PKS fuel in term of calorific value in designing and enhancing the performance of a micro power plant for producing superheated steam.

ISSN No. 2454-6194 | DOI: 10.51584/IJRIAS |Volume X Issue XI November 2025

There are several technologies employed that enable biomass such as PKS to be useful for generating heat energy for domestic and industrial consumption. In some cases excess energies produced were exported to enhance foreign exchange in the recent past. Selected relevant studies on combustion of biomass on grate and fluidized bed power plants are Pichet and Vladimir, (2014); Oladosu (2016); Yusniati et al. (2018); and Oladosu *et al.* (2017). Findings from those studies showed that they concentrated more on optimizing PKS biomass performance but they are deficient in optimizing actual plant efficiency. This is the gap this study posed to bridge.

The consideration of PKS fuel in the design of micro steam power plant would lower the cost of fuelling (Kareem and Babatunde, 2018; Kareem et al., 2018 a, b, c; Elefe et al. 2024). This study concentrated on how to enhance the efficiency of whole power plant through reduction of heat losses and optimal design of components.

RESEARCH METHODOLOGY

Micro Steam Generator Design Concept

The steam generator used was designed to have water tank (reservoir) called primary water/feeder supported by a frame called tank stand. This primary feeder (tank) (ϕ 45 cm x 30 cm) is water fed by gravity from a reservoir tank placed on building top/ tower by gravity. Primary tank water level is controlled mechanically using floating mechanism. A metallic ladder is designed on tank stand to check primary tank's water level if desired. The primary tank is made to allow the flow water into secondary tank (30 cm x 15 cm) (reservoir) through half inch (½'') diameter metallic pipe whose flow rate is mechanically regulated/controlled using half inch (½'') diameter metallic ball gauge valve. The secondary tank is designed to have floating mechanism to regulate water level in the tank. The release of water from secondary tank into the boiler vessel (30 cm x ϕ 30 cm) is moderated by a half inch (½'') diameter metallic ball gauge value and a half inch (½'') diameter non-return valve. Water inlet orifice is located 18 cm from the 30 cm diameter base of the cylindrical vessel. A half inch diameter non-return value is incorporated to prevent backflow of water/steam from cylindrical vessel to the secondary tank during combustion process. The vessel is firmly sealed at the top using heat resistant leather insulator and secured with six-number 19 mm bolts/nuts to prevent heat loss. A ½'' orifice was made close to the base of the vessel and piped to allow evacuation of leftover water through a ½'' ball gauge fixed to its end after operation. Three equal lengths (90 cm) and diameters (½'') stainless helical-shaped risers are welded to balance on the top of the cylindrical vessel and made to converge at 90 cm from the cylindrical vessel's top using a small stainless cylindrical-shaped (ϕ 6 cm x 5 cm), A single stainless coiled (½'' diameter) super-heater emerges from the stainless cylindrical-shaped (ϕ 6 cm x 5 cm) and terminated at a small steam tank (ϕ 6 cm x 10 cm. The steam tank had two outlets: one for steam regulator (incorporated with ½'' ball gauge value) and testing steam presence, and for evacuating condensed water after operation; while second outlet served as measurement window (steam pressure and temperature) and steam supply channel for powering purpose. The furnace is provided combustion using biomass PKS as fuel. Furnace is designed and insulated to prevent heat losses from the compartment using combined refractory brick, fibre glass and synthetic leaders as insulators. Regulated primary and secondary air flow systems are provided using regulated fanning mechanism (based on bimetallic strip controller) for effective heating and to facilitate evenly temperature distribution across the combustion chamber. The line diagram of the design is shown in Fig. 1.

ISSN No. 2454-6194 | DOI: 10.51584/IJRIAS |Volume X Issue XI November 2025

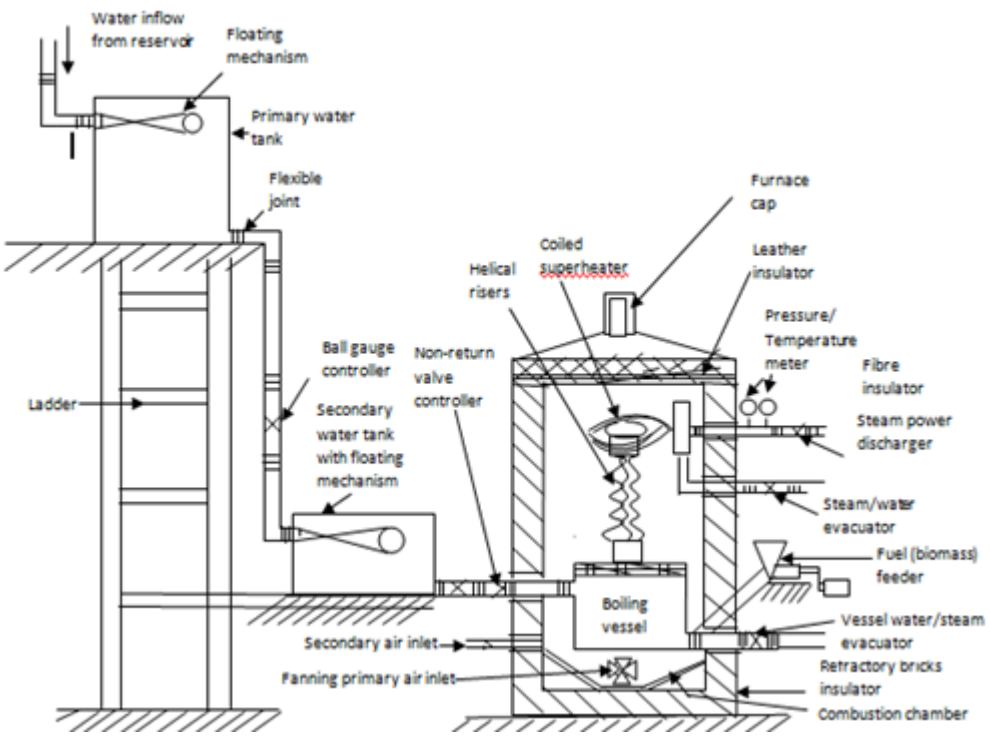

Fig.1. Micro Steam Generator Design Concepts

Design Calculations

Steam power plant/boiler system design and operation

The steam power plant/boiler has the following design and operation conditions:

i. Water-tube/steam generator-type.

ii. Operating pressure range.

iii. Superheated steam quality.

iv. Feed water at room temperature.

v. Palm kernel (biomass) shell (PKS) fuelled with calorific value 18MJ/kg

vi. Assumed boiler system efficiency of 79% (Lawal, 2025)

Assumptions made in design calculations are:

i. Steady-state operation for the boiler system.

ii. Negligible heat losses and within the limit of the boiler's efficiency.

iii. Properties of PKS as fuel (e.g. calorific value, moisture content) were not changed significantly during usage.

iv. Specific design parameters for boiler remain constant (e.g. heat transfer area, tube diameter).

v. Thermodynamic property data for water and steam from steam tables are used.

The design focus is to obtain the following performance parameters

ISSN No. 2454-6194 | DOI: 10.51584/IJRIAS |Volume X Issue XI November 2025

i. The required steam flow rate based on the system's demands.

ii. The required heat transfer rate to achieve the desired steam conditions.

Design of 5-10 kW micro steam power plant/generator

Micro steam power plant considered were within the range of 5-45 kW (Oladosu et al., 2018). Five-Ten (5-10) kW micro steam power plant was selected for this study. For a superheated steam generator of 10 kW, with operating pressure P_o range of 0.45-4.5 MPa, feed water temperature T_f of 34^{o}C under atmospheric pressure, palm kernel shell (PKS) of calorific value C_v 18 MJ used as fuel, assuming boiler efficiency of 79%, and tube diameter of 12.7 mm. Design parameters for the steam flow rate, heat transfer rate, boiler outlet steam temperature and pressure, steam flow velocity through the tube (pipe).

Design for Mechanical and Physical Properties

In order to estimate the maximum load F on the stand of the furnace/boiler casing, the total mass m_i on the mild steel stand was computed first:

$$m_i = m_c + m_r + \emptyset m_c \quad (1)$$

Where, m_c, the mass of boiler casing/chamber; m_r, the mass of refractory brick (insulation) lining on the boiler casing; $\emptyset$ is the fractional factor of casing mass attributed to the boiler elements (cover, fan, downcomer, steam drum, riser, super-heater, temperature, pressure and flow rate gauges, PKS feeder, water feeder, etc).

m_c was estimated using density, ρ_c – volume, V_c relationship for mild steel plate of standard thickness 5 mm and density , 7850 kg/m^3 as

$$m_c = \rho_c V_c \quad (2)$$

Based on designed cuboids furnace/boiler casing of 1000 x 1000 x 2000 mm by 5 mm thickness, volume of the mild steel component V_c of the cuboids;

$$V_c = V_{ce} - V_{ci} \quad (3)$$

Where V_{ce}, the external volume of the cuboids; and V_{ci} is the internal volume of the cuboids.

That is;

V_c= (1 m x 1 m x 2 m) – (0.99 m x 0.99 m x 2 m) = 2 m^3 -1.9602 m^3

V_c=0.0398 m^3

Therefore, m_c from Eqn. (32) revealed as

m_c= 7850 kg/m^3 (0.0398 m^3) =312.43 kg

By assuming a factor of 0.9 for other attached elements, m_{ca}, then;

$m_{ca} = 0.9m_c$=0.9(312.43) = 281.187 kg

Refractory brick made up of 60% kaolin by weight (particle size 2.5mm, ball clay (particle size 1mm) and saw dust (particle size 2.5mm): 30% and 10% respectively used based on Oladosu (2016) specifications. Size 1.8 kg (275mm x 130mm x 60mm) each of 150 refractory bricks, rectangular in shape was used to insulate the furnace/boiler casing to reduce heat loss. Therefore, total mass of refractory bricks m_r was estimated as;

m_r = 1.8 kg (150) = 270 kg

ISSN No. 2454-6194 | DOI: 10.51584/IJRIAS |Volume X Issue XI November 2025

Total mass on the stand was computed using Eqn. (31) as

m_i = (312.43 + 281.187 + 270) kg = 863.617 kg.

The m_i on the stand was approximated to 1000 kg (1 ton) due to other masses that were unaccounted for and may come during welding, fabrication, and assembly process.

The stress, strain on a standard angle mild steel stand of length 1m and thickness 10 mm (0.01 m) under a distributed load of 1ton (comprised mild steel and refractory bricks) were computed under the following design parameters:

i.The angle mild steel is a standard equal angle section (50 x 50 x 5 mm-50 x 50 x 10 mm) was used as stand/support.

ii.. The distributed load of 1 ton (1000 kg or 9806.65 N was applied uniformly along the length of the angle.

iii.. The angle is simply supported at both ends.

iv. The material properties of mild steel used are: Young's modulus (E) taken to be 200 GPa (200,000 N/mm²) and Yield strength of 250 MPa (250 N/mm²)

v.. The load assumed to be applied perpendicular to one of the legs.

Total Load F is computed as product of mass (m_i) of the mild steel/refractory brick and acceleration due to gravity;

$$F = m_i g \quad (4)$$

F =1000kg x 98.07 m/s^2

F = 9807 N

For a standard equal angle section (50 x 50 x 5 mm), the moment of inertia (I) about the horizontal x-x axis is taken to be 10.96 cm⁴ or 109600 mm⁴.

The Section Modulus (Z)

$$Z = I / y \quad (5)$$

where y is the distance from the neutral axis to the extreme fiber.

For a standard equal angle section, y ≈ 25 mm (half the width of the angle).

Z ≈ 109600 mm⁴ / 25 mm ≈ 4384 mm³

Maximum Bending Moment (M) for a simply supported beam with a uniformly distributed load from;

$$M = F \times L / 4 \quad (6)$$

= 9807 N × 1000 mm / 4

= 2451750 Nmm

The corresponding Maximum Stress (σ) obtained from ;

$$\sigma = M / Z \quad (7)$$

ISSN No. 2454-6194 | DOI: 10.51584/IJRIAS |Volume X Issue XI November 2025

σ = 2451750 N·mm / 4384 mm³

≈ 559.3 N/mm²

≈559.3 MPa

The strain (ε) also obtained from;

$\varepsilon = \sigma / E$ (8)

= 559.3 N/mm² / 200000 N/mm²

≈ 0.0028

≈ 0.28%

From Eqn. (7) the stress σ obtained (559.3 MPa) exceeds the yield strength F_{os} of mild steel (250 MPa), which means the material may undergo plastic deformation or failure under this load. Therefore, a safety factor applied to ensure the material remains within its elastic limit to prevent design failure.

Then, the Factor of Safety (F_{os}) for the yield strength of mild steel of (250 MPa) under maximum stress σ obtained from;

$F_{os} = F_{os} / \sigma$ (9)

F_{os}= 250 MPa / 559.3 MPa

F_{os}≈ 0.447

The outcome F_{os}≈ 0.447 showed that the design is not safe, therefore can fail under this load.

Then the corresponding deflection (δ) for the simply supported beam with a uniformly distributed load considered;

$\delta = (5 \times F \times L^3) / (384 \times E \times I)$ (10)

= (5 × 9807 N × (1000 mm)³) / (384 × 200000 N/mm² × 109600 mm⁴)

δ ≈ 5.83 mm

The Shear Stress (τ) also obtained from Eqn. (10), where area A_c is a cross sectional area of the mild steel;

$\tau = F / (2 \times A_c)$ (11)

τ = 9807 N / (2 × 50 mm × 5 mm)

τ ≈ 19.61 MPa

The summary of the outcomes of the mechanical and physical properties obtained for a 50 x 50 x 5 mm angle mild steel used as support stand/table (1 m x 1 m) for the furnace chamber/casing of the boiler is shown in Table 1.

Similar procedures were applied to estimate the stated parameters with the thickness doubled to 10 mm.

Moment of Inertia (I) for a standard equal angle section (50x50x10 mm), about the x-x axis is approximately 43.84 cm⁴ or 438400 mm⁴ .

ISSN No. 2454-6194 | DOI: 10.51584/IJRIAS |Volume X Issue XI November 2025

Section Modulus (Z) is

$$Z = I / y$$

where y is the distance from the neutral axis to the extreme fiber. For a standard equal angle section considered, $y \approx 25$ mm (half the width of the angle).

$Z \approx 438400$ mm⁴ / 25 mm ≈ 17536 mm³

The Maximum Bending Moment (M) for a simply supported beam with a uniformly distributed load;

$$M = F \times L / 4$$

= 9807 N × 1000 mm / 4

= 2451750 N mm

The Maximum Stress (σ)

$$\sigma = M / Z$$

= 2451750 N mm / 17536 mm³

≈ 139.8 N/mm² or 139.8 MPa

The Strain (ε)

$$\varepsilon = \sigma / E$$

= 139.8 N/mm² / 200000 N/mm²

≈ 0.0007 or 0.07%

Factor of Safety (F_{os})

F_{os}= 250 MPa / 139.8 MPa

≈ 1.79

The Deflection (δ) $F_{os}$for a simply supported beam with a 9807 N uniformly distributed load:

$\delta = (5 \times F \times L^3) / (384 \times E \times I)$

= (5 × 9807 N × (1000 mm)³) / (384 × 200000 N/mm² × 438400 mm⁴)

≈ 1.46 mm

The Shear Stress (τ)

$\tau = F$ / (2 × Area)

= 9807 N / (2 × 50 mm × 10 mm)

≈ 9.81 MPa

ISSN No. 2454-6194 | DOI: 10.51584/IJRIAS |Volume X Issue XI November 2025

The physical properties evaluation with 5-10 mm thick mild steel with refractory brick lagging of thickness of 60 mm, while thermal conductivity of mild steel is 50 W/m K and thermal conductivity of refractory brick is 0.5 W/m K is sustainable.

In calculating overall heat transfer coefficient H_{tc}, the thermal resistance of both the mild steel and the refractory brick lagging was considered.

Thermal Resistance of Mild Steel R_{ms} obtained from ratio of mild steel thickness (t_{ms}) and thermal conductivity (S_{tc});

$R_{ms} = t_{ms}/S_{tc}$

= 0.01 m / 50 W/m K

= 0.0002 m²K/W

The corresponding heat flux q_{ms} with ambient temperature 22 ^{o}C and designed temperature of 400 ^{o}C was estimated from

$q_{ms} = \partial T/R_{ms}$

$q_{ms} = (22 - 400)^{o}$C /0.0002 m²K/W = 378K/0.0002 m²K/W=1,890,000 W/m^2

q_{ms} =1,890,000 W/m^2 =1.89 W/mm^2

The thermal resistance of refractory brick (R_{rb}) was estimated as the ratio of refractory brick thickness $t_{rb}$and that of its thermal conductivity R_{tb}as;

$R_{rb} = t_{rb}/R_{tb}$

= 0.06 m / 0.5 W/mK

= 0.12 m²K/W

The corresponding heat flux q_{rb} with ambient temperature 22 ^{o}C and designed temperature of 400 ^{o}C was estimated from

$q_{rb} = \partial T/R_{rb}$

$q_{rb} = (22 - 400)^{o}$C /0.12 m²K/W = 378K/0.12 m²K/W=3,150 W/m^2

q_{rb} =3,150 W/m^2 = 0.003150 W/mm^2

Overall Thermal Resistance (R_T) was obtained from;

$R_T = R_{ms} + R_{rb}$

= 0.0002 m²K/W + 0.12 m²K/W

≈ 0.1202 m²K/W

Overall Heat Transfer Coefficient, H_{tc}

H_{tc} = 1 / R_T

= 1 / 0.1202 m²K/W

ISSN No. 2454-6194 | DOI: 10.51584/IJRIAS |Volume X Issue XI November 2025

≈ 8.32 W/m² K

The corresponding heat flux q_{ms} with ambient temperature 22 ºC and designed temperature of 400 ºC was estimated from

$$q_T = \partial T / R_T$$

$q_T = (22 - 400)$ºC /0.1202 m²K/W = 378K/0.1202 m²K/W=3,144.76 W/m^2

q_T =3,144.76 W/m^2 ≈ 0.003145 W/mm^2

If the mild steel thickness is 5 mm (0.005 m), then,

$R_{ms} = t_{ms}/S_{tc}$

= 0.005 m / 50 W/m K

= 0.0001 m²K/W

Overall Thermal Resistance (R_T) would be;

$R_T = R_{ms} + R_{rb}$

= 0.0001 m²K/W + 0.12 m²K/W

≈ 0.1201 m²K/W

Then, Overall Heat Transfer Coefficient H_{tc} would be;

H_{tc} = 1 / R_T

= 1 / 0.1201 m²K/W

≈ 8.326 W/m² K

The corresponding heat flux q_{ms} with ambient temperature 22 ºC and designed temperature of 400 ºC would be

$$q_T = \partial T / R_T$$

$q_T = (22 - 400)$ºC /0.1201 m²K/W = 378K/0.1201 m²K/W=3,147.377W/m^2

q_T =3,147.377 W/m^2 ≈ 0.003147 W/mm^2

The outcomes showed that refractory brick lagging significantly reduces the heat transfer rate due to its low thermal conductivity while there is no significant change in heat transfer rate reduction in usage of mild steel plate of 5 mm and 10 mm thickness. Hence, the choice of mild steel plate of 5 mm thickness or less would be economical.

In the case of down comer, riser and superheater, stainless steel material was used. By assuming thermal conductivity k_{ss} of 16.2 W/mK (range from 16.2- 22.6 W/mK, 100ºC (373K)- 500 ºC (773 K)) for popular stainless steel 304 with a thickness L_{ss} of 0.003m (3 mm), heat flux q_{ss} for stainless steel heated from ambient (outside) temperature of 22 ºC to design temperature of 450 ºC can be obtained using Fourier's law from;

$$q_{ss} = -k_{ss}\partial T / L_{ss}$$

$$q_{ss} = -16.2\, W/mK\ (-428\, K)/0.003$$

ISSN No. 2454-6194 | DOI: 10.51584/IJRIAS |Volume X Issue XI November 2025

$$q_{ss} = 2{,}311{,}200\ W/m^2 \approx 2.3112\ W/mm^2$$

The thermal resistance R_{ss} can be calculated from

$R_{ss} = L_{ss}/k_{ss}$

$R_{ss} = 0.003\ m/16.2\ W/mK \approx 0.000185\ m^2K/W$

Then, Overall Heat Transfer Coefficient H_{ss} would be;

$H_{ss} = 1 / R_{ss}$

= 1 / 0.000185 m²K/W

≈ 5,405 W/m² K

The hydrostatic pressure P_{hs}, on the reservoir cylinder is obtained using Eqn. 12 as;

$$P_{hs} = \rho_w g h_w \quad (12)$$

Where ρ_w is the desity of water in the cylinderial vessel, g, is the acceleration due to gravity, and h_w is the possible maximum height of water in the vessel.

For the cylindrical basin (reservoir) design,

$$P_{hs}{}^{cylinder} = \rho_w g h_w = 1000kg/m^3(9.807m/s^2)(0.3m) = 2{,}942N/m^2$$

For the cuboid basin (feeding tank) design,

$$P_{hs}{}^{cuboid} = \rho_w g h_w = 1000kg/m^3(9.807m/s^2)(0.15m) = 1{,}471N/m^2$$

For the designed volume, V_w;

$V_{wc} = \pi r^2 h_w = \frac{22}{7}(0.15)^2\ 0.3\ = 0.02121525m^3 \approx$ 21.22 litres

By considering density of water ρ_w as 1000 kg/m^3, then, mass of water m_{wc} is estimated as;

$m_{wc} = V_{wc}\rho_w = 0.02121525m^3(1000kg/m^3) \approx$21.22kg

Force acting on the cylindrical water tank (reservoir) stand, F_{wc}

$$F_{wc} = m_{wc} g = 21.22(9.807) = 196.14N$$

Equivalent volume of mild steel container (density ρ 7850 kg/m^3) and thickness (5 mm) for the cylindrical water reservoir tank was estimated from

$$V_{wrm} = \pi r^2 h_w - \pi r'^2 h_w \quad (13)$$

$$V_{wrm} = 0.02121525m^3 - \frac{22}{7}(0.145)^2\ 0.3 = 0.001392\ m^3$$

$$m_{wrm} = \rho V_{wrm} = 7850(0.001392) = 10.92724\ kg$$

Total weight;

$$F_{wrT} = F_{wc} + F'_{wc} = 196.14\ N + 10.92724(9.807) \approx 315.27N \quad (14)$$

ISSN No. 2454-6194 | DOI: 10.51584/IJRIAS |Volume X Issue XI November 2025

Stress σ'_{wrT} exerted on the stand by the cylinder reservoir; was obtained as the ratio of total force applied F_{wrT} and the base area A_{wrb};

$$\sigma'_{wrT} = \frac{F_{wrT}}{A_{wrb}} = \frac{315.27}{\frac{22}{7}(0.15)^2} = \frac{315.27}{0.07071429} = 4{,}458.36\ N/m^2 \quad (15)$$

Similarly, for the cuboids water feeding tank

$V_{wc} = lbh_w = 0.276(0.1835)\ 0.15 = 0.0075969m^3 \approx 7.6$ litres

Then equivalent mass of water (kg) m_{wc} and weight F_{wc} is respectively estimated as;

$m_{wc} = V_{wc}\rho_w = 0.0075969m^3(1000kg/m^3) \approx 7.6$kg

$$F_{wc} = m_{wc}g = 7.6(9.807) = 74.5332N \approx 74.5N$$

Equivalent volume of mild steel container (density ρ 7850 kg/m^3) and thickness (5 mm) for the cuboids water feeding tank was estimated from

$$V_{wcm} = lbh_w - l'b'h_w' \quad (16)$$

$$V_{wcm} = 0.276(0.1835)0.15 - 0.771(0.1785)0.15 = 0.000340875m^3$$

$$m_{wcm} = \rho V_{wcm} = 7850(0.00034087) = 2.676\ kg$$

Total weight;

$$F_{wcT} = F_{wc} + F'_{wc} = 74.5332N + 2.676(9.807) \approx 100.78N \quad (17)$$

Stress σ'_{wcT} exerted on the stand by the cuboids; was obtained as the ratio of total force applied F_{wcT} and the base area A_{wcb};

$$\sigma'_{wcT} = \frac{F_{wcT}}{A_{wcb}} = \frac{100.78}{0.276\ (0.1835)} = 1{,}989.9N/m^2 \quad (18)$$

Total stress on the stand σ_{crT};

$$\sigma_{crT} = \sigma'_{wrT} + \sigma'_{wcT} = 4{,}458.36\ N/m^2 + 1{,}989.9N/m^2 \quad (19)$$

$$\sigma_{crT} = 6{,}448.26\ N/m^2$$

In analyzing the stress exerted by the PKS feeding hopper on its stand, PKS feeding rate (0.000703 kg/s ≈ 2.5308 kg/hr) and density of PKS (350-400 kg/m^3, 375 kg/m^3 on average) were considered. On this basis, volumetric flow rate, $\mathcal{V}_{pks}$

$$\mathcal{V}_{pks} = \frac{\dot{m}_{pks}}{\rho_{pks}} \quad (20)$$

$\dot{m}_{pks}$ is the mass flow rate of PKS while ρ_{pks} is the PKS average density.

$$\mathcal{V}_{pks} = \frac{2.5308\ kg/h}{375\ kg/m^3} = 0.00675\ m^3/h$$

Then, the volume of the pyramid container V_p to fill with PKS was obtained using frustum of a pyramid formula as;

$$V_p = \frac{1}{3}abh - \frac{1}{3}a'b'h' \quad (21)$$

ISSN No. 2454-6194 | DOI: 10.51584/IJRIAS |Volume X Issue XI November 2025

$$V_p = \frac{1}{3}(0.152)(0.152)(0.156) - \frac{1}{3}(0.04)(0.03)(0.042)$$

$$V_p = 0.001201408\, m^3 - 0.0000224\, m^3 = 0.001179008\, m^3$$

Then, the volume of the cuboids component V_c to fill with PKS was obtained using;

$$V_c = l_c b_c h_c = 0.04(0.03)0.042 = 0.0000504\, m^3$$

The volume of the cylindrical component V_y to fill with PKS was obtained using;

$$V_y = \pi {r_y}^2 h_y = \frac{22}{7}(0.015)^2(0.17) = 0.0001202198\, m^3$$

Total maximum possible PKS volume in the hopper container, V_{pks} was estimated by;

$$V_{pks} = V_p + V_c + V_y = 0.0013496278 \approx 0.00135\, m^3 \quad (22)$$

Actual size that took care of scaling in the AutoCaD design V_{Apks} was computed as;

$$V_{Apks} = 2V_{pks} = 2(0.00135) = 0.0027\, m^3$$

Time taken $t_f$to fill the hopper volume $0.0027\, m^3$ to the brim was estimated as;

$$t_f = \frac{V_{Apks}}{\mathcal{V}_{pks}} = \frac{0.0027 m^3}{0.00675\, m^3/h} = 0.4h = 24\, mins. \quad (23)$$

Total mass of the PKS in the hopper m_{pks} was computed using,

$$m_{pks} = \rho_{pks}(V_{pks}) = 375\frac{kg}{m^3(0.0027\, m^3)} = 1.02\, kg$$

Also, estimation of mass of the mild steel of density ($\rho_{ms} = 7850\, kg/m^3$) PKS feeding hopper having pyramidal and cuboids thickness of (5 mm), and cylindrical section thickness of 10 mm (to compensate for the auger shaft) was carried out, thus:

$$V'_p = \frac{1}{3}(0.147)(0.147)(0.156) - \frac{1}{3}(0.035)(0.025)(0.042)$$

$$V'_p = 0.001123665 - 0.00001225 = 0.001111418\, m^3$$

Similarly,

$$V'_c = 0.035(0.025)0.042 = 0.00003675\, m^3$$

$$V'_y = \frac{22}{7}(0.005)^2 0.17 = 0.0000133578\, m^3$$

$$V'_{pks} = V'_p + V'_c + V'_y = 0.0011615258\, m^3$$

Actual size that took care of AutoCaD scaling V'_{Apks} was computed as;

$$V'_{Apks} = 2V'_{pks} = 2(0.0011615258\, m^3) = 0.0023230516\, m^3$$

Volume differential V_d

$$V_d = V_{Apks} - V'_{Apks} = 0.0027\,m^3 - 0.0023230516\,m^3 \approx 0.000377\,m^3 \quad (24)$$

Therefore, the mass of steel m_s is given as (with density of steel ρ_s);

$$m_s = V_d\rho_s = 0.000377\,m^3(7850\,kg/m^3) = 2.942kg$$

Total mass m_{sT}

$$m_{sT} = m_s + m_{pks=}1.02 + 2.942 = 3.962\,kg \quad (25)$$

Hence, total weight on the hopper stand F_{hs};

$$F_{hs} = 3.962\ (9.807) \approx 38.85N$$

By assuming that maximum stress was acted on the neck portion Area of the hopper (A_{hs}), then stress on the hopper stand σ_{hs} is given as;

$$\sigma_{hs} = \frac{F_{hs}}{A_{hs}} = \frac{38.85N}{0.04\ m\ (0.03\ m)} = 32{,}375\ N/m^2 \quad (26)$$

Control of air blower fan to aid combustion of PKS was facilitated using Direct Current (DC), 12 Volts Electronic Temperature Controller (ETC) programmable to -50 to 110ºC Heating/Cooling Thermostat Control Switch Module Waterproof with Sensor Probe Dual Colour LED Display Monitor.

The location of the sensor was established using dimensional similarity analysis based on ratio of maximum temperature of sensor T_{ms} with that of maximum temperature of furnace T_{mf} which is equivalent to the ratio of distance of sensor location from the tip of the air blower fan d_{fs} to the center distance of the furnace/burner d_{fb};

That is;

$$\frac{T_{ms}}{T_{mf}} = \frac{d_{fs}}{d_{fb}} \quad (27)$$

Then, sensor location distance on the air blower fan,

$$d_{fs} = \frac{T_{ms}}{T_{mf}}d_{fb} \quad (28)$$

Therefore, provided that there is no heat loss;

$$d_{fs} = \frac{110^oC}{1200^oC}\left(\frac{0.181m}{2}\right) = 0.0083\,m$$

The actual distance after considering design scale, d'_{fs};

$$d'_{fs} = 0.0083\ (6) = 0.0498\,m = 49.8\,mm$$

Furnace sieve for ash release from the burnt PKS fuel was designed with sieve size of 0.0028 m by 0.00204 m for easy passage of ashes from the combustion chamber to the ash collector/ basin located at the base, below the furnace/heating chamber.

Micro Steam Plant Design Modeling and Simulation

Each of the components was modeled using Solidworks CAD software and then analyzed (simulated) using Ansys software to determine their design integrity. Isometric projection model of the designed micro power plant using Solidworks/ AutoCAD tools is shown in Figure 2. Thermal (physical) and mechanical properties)

ISSN No. 2454-6194 | DOI: 10.51584/IJRIAS |Volume X Issue XI November 2025

analyses were used to determine the behavior of the model (component) with respect to the temperature differences and the load applied, respectively. First, the static structure analysis of the component was carried out based on the load capacities. Second, the total and dimensional deformation, strain, and (Von- Misses) stress equivalents were determined, and third, the thermal analysis of the steam generating furnace/chamber was carried out.

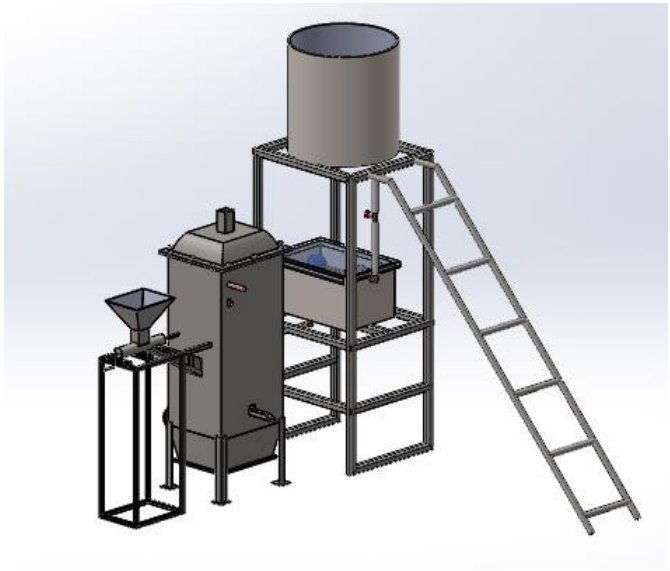

Figure 2: Isometric view of the Steam Plant Model.

The list of material standard mechanical properties used for the analysis is shown in Table 2.

Table 2 Material Selection

Material Properties	Low Carbon Steel (Mild Steel)	Refractory bricks/Marble	Stainless steel (304)	Palm Kernel Shell (PKS)
Density (kg/m^3)	7850	2780	7720	350-400 (375)
Young's modulus (Pa)	2.1e+11	5.926e+11	2e+11	
Poisson's ratio	0.29	0.175	0.28	
Tensile Yield stress (Pa)	3.29e+08	3e+6	3e+8	
Tensile Ultimate stress (Pa)	4.4e+08	5e+6	6e+8	
Specific heat capacity, J/kg/C	485	870	688	
Thermal Conductivity, W/m/C	50	5.48	16.2	
Thermal Yield stress, Pa	3.29e+8	7.75e+6	2.91e+8	

RESULTS AND DISCUSSION

Design and simulation Results of components

The design results of the mechanical and physical properties obtained for the furnace chamber/casing of the boiler are shown in Table 3. The results showed that angular mild steel stand of 5 mm thickness cannot withstand the load due to low factor of safety (0.447). Redesign results using angular mild steel (10 mm) showed a good factor of safety of (1.79), which is highly adequate to support the plant's chamber. This outcome indicated that

any angular mild steel of diameter ranging 5 -10 mm should be adequate as support for the plant. All other designed parameters (stress, strain, deflection, and thermal resistance) were within the acceptable standard, this portrayed design adequacy.

Table 3 also shows the outcomes of applications of conventional and simulated design methods. It can be clearly shown that the mechanical, physical thermal and simulation outcomes were adequate for all the parameters under consideration for the micro power plant.

Table 3. Furnace Chamber designed by conventional and simulation methods

Designed Properties	Conventional: Mild steel of 5 mm thickness	Conventional: Mild steel of 10 mm thickness	Simulation: Mild steel of 10 mm thickness
Load, F, N	9807	9807	9807
Moment of inertia (I), mm⁴	109600	438400	
Section Modulus (Z), mm³	4384	17536	
Maximum Bending Moment (M), Nmm	2451750	2451750	
Maximum Stress (σ), MPa	559.3	139.8	497
Strain (ε) %	0.28%	0.07%	0.0-1.69%
Factor of Safety (F_{os})	0.447	1.79	0.6-15
Deflection (δ), mm	5.83	1.46	0.0-1.8
Shear Stress (τ). MPa	19.61	9.81	9.81
Density, ρ, kg/m³	7850	7850	7850
Thermal conductivity, C_T, W/m·K	50	50	50
Specific heat capacity, C_S J/kg·K	500	500	500
Thermal Resistance of Mild Steel R_{ms}, m²K/W	0.0001	0.0002	0.0002
Thermal Resistance of refractory brick (R_{rb}), m²K/W	0.12	0.12	0.12
Thermal Resistance of mild steel and refractory brick (R_{rb}), m²K/W	0.1201	0.1202	0.1202
Total Heat Flux of combined mild steel and refractory bricks at ∂T (22°C-400°C (378 °C=378K) W/mm^2	0.00315	0.00314	2.4008 x 10^{-12} – 17.066

ISSN No. 2454-6194 | DOI: 10.51584/IJRIAS |Volume X Issue XI November 2025

The design results of other supporting components using conventional and simulation methods are respectively presented in Table 4.

Table 4 Supporting Components designed by conventional and simulation methods

Design Parameters	Conventional 5mm thickness mild steel	Conventional 3mm stainless steel (304)	Simulation
Water tanks (feeding /reservoir) support/stand		-	
Load, F, N	416	-	
Maximum Stress (σ), kPa	6.44826	-	370-3490.7
Strain (ε) %	0.07	-	0.0-1.69
Factor of Safety (F_{os})	1.78	-	0.6-15
Deflection (δ), mm	1.45	-	0.0-1.8
Density, ρ, kg/m³	7850	-	7850
PKS Fuel feeding hopper support/stand			
Load, F, N	50	-	
Deformation	0.0	-	0-0.001343
Elastic strain	0.0	-	0-0.00002384
Maximum stress kPa	32.375	-	81.92-4970.9
Factor of Safety (F_{os})	1.78	-	0.-15
Hopper Auger /Shaft			
Deformation (mm)	0	-	0-0.00025118
Elastic strain	0	-	0.0-0.0024396
Factor of safety	1.5	-	0.65-15.0
Maximum Stress, kPa	32.375	-	0-4970.90
Thermal analysis of the furnace chamber compoents			
Steam Chamber analysis: Heating effect and retention , ^{o}C	400	-	0-1200
Steam Chamber Total heat flux, W/mm^2	0.00315	-	2.4008 x 10^{-12} -17.066

Boiling vessel/ down-comer under thermal loading, ^{o}C		450	450-1403.2
Total heat flux vessel/down-comer/risers, W/mm^2	-	2.31	1.9971 x 10^{-15} - 56.653
Thermal Resistance of Stainless Steel R_{ms}, m^{2}K/W	-	0.000185	-
Air Blower Sensor location (mm)	49.8	-	-

Design Validation by Simulation Analysis of the Plant's Components

The outcomes of the simulation analyses of the components of the micro steam power plant are shown in Tables 3 and 4. For example, the results of the total deformation of the water tank support showed that it was within the acceptable range (Figure 3).

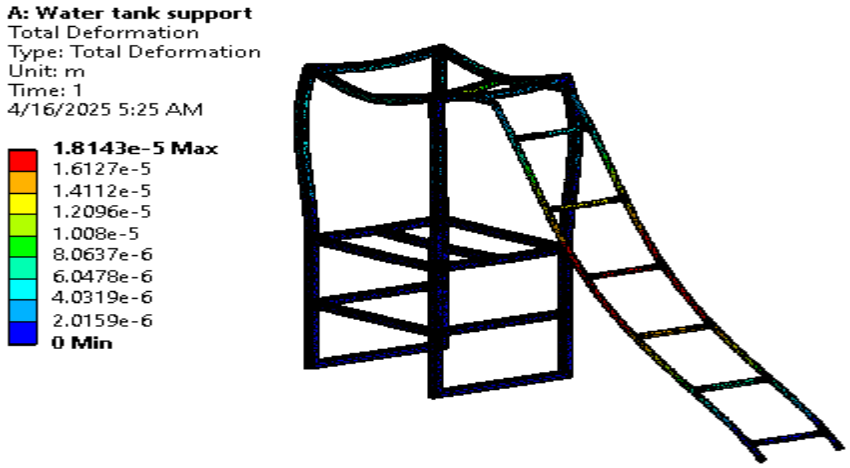

Figure 3 Total deformation of the water tank support.

Figure 3 shows the response of the frame to the elastic strain, which indicated that designed value was within the range (Tables 3 and 4). Simulation analysis results on stresses, strains, factor of safety on water tank support, water storage tank, PKS feeding hopper, and other components are presented in Tables 3 and 4.

Material selection for the thermal simulation analysis of the designed steam power plant is presented in Table 5.

Table 5: Material selection for thermal simulation of designed power plant components

Material Properties	Mild steel	Marble	Stainless Steel (304)
Density (Kg/m^3)	7850	2780	7720
Thermal conductivity (W/m/C)	52	5.48	16.2
Specify heat, Co (J/Kg/C)	485	870	488
Poisson Ratio	0.29	0.175	0.28
Young Modulus (Pa)	2.1E+11	5.926E+10	2E11
Thermal Yield stress	3.29E+8	7.75E+6	2.91E8

ISSN No. 2454-6194 | DOI: 10.51584/IJRIAS |Volume X Issue XI November 2025

The results generated for the steam chamber for temperature analysis are presented in Figure 4. It was revealed that designed temperature of 0- 400^{o}C was within the acceptable range and far from maximum tolerable temperature of 1200^{o}C. Besides, the results indicated that there are more heating effect happening inside the chamber and the heat loss is negligible, since the outside seems to show a blue colour, showing that the material can withstand the thermal effect even beyond 1200^{o}C.

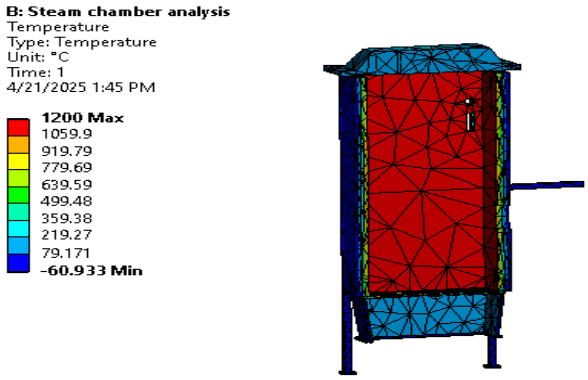

Figure 4: Temperature difference inside the Steam Chamber.

The outcomes of other simulation results indicated that chamber accommodate the designed heat flux (0.00315 W/mm^2). System has ability to superheat from 450 to 1140.2 ^{o}C based on the simulation results is an indication that the maximum designed superheated temperature of 400- 450 ^{o}C could be accommodated. These simulation outcomes have validated that of the conventional design, and hence workable. Comparative results of the design efficiency (79%) with the existing power plants (Elefe *et al.*, 2024; Oladosu *et. al*., 2017; Oladosu, 2016) showed a good improvement (12 %) as indicated in Table 6 and close to the standard expected value (85%). This is a novel contribution in the area of micro steam power plant development.

Table 6: Efficiency Comparison with Past Designs

Studies	Elefe *et al.*, 2024	Oladosu *et. al.*, 2017	Standard Rated Design Capacity (Oladosu, 2016)	This study	Improvement over Elefe, *et al*, 2024)
Plant efficiency (%)	67	59	85	79	12

CONCLUSION

A PKS-fired 5-10 kW micro power plant has been designed, modeled and simulated to produce superheated steam for domestic and SMEs consumption. The design outcomes were compared with those obtained from the micro power plants designed in the past. Sustainable power output at optimal design parameters were achieved due to enhancement of efficiency across the plant's components. Reduction of heat losses at optimal design of components was also evidenced. Other conclusions made from the results obtained are itemized as follows:

i. Temperature range of 220-400 ^{o}C has effectively enhanced the performances of the designed 5- 10 kW micro steam power plants.

ii. Temperatures (pressures) of 250 ^{o}C (2.5 MPa), and 220 ^{o}C, 250 ^{o}C (0.38 MPa, 2.5 MPa) resulted to the highest seam mass flow rate of 0.00452 kg/s and 0.00181 kg/s respectively for the steam power plant of 10 kW and 5 kW capacity under similar PKS feeding rate of 0.000703 kg/s and 0.000352 kg/s, respectively.

iii. For highest steam flow velocities design (15.5 m/s, 16.5 m/s) temperatures (pressures) should be maintained at 400 ^{o}C (0.45 MPa) and 250 ^{o}C (2.5 MPa) respectively for the 10 kW and 5 kW power plants.

iv. For safety and economy of operation, running at the lowest possible temperatures (pressures) of 235 ^{o}C (0.35 MPa) and 235 ^{o}C (0.35 MPa) will be sufficient in both plants (10 kW and 5 kW) for generating acceptable steam mass flow rates (0.00357 kg/s, 0.00178) and steam flow velocities (14.87 m/s, 7.43 m/s), respectively.

v. Temperature (pressure) range of 220 - 400 ^{o}C (0.35-4.2 MPa) was adequate for the designed 10 kW and 5 kW steam micro power plants.

vi. Angular mild steel stand of 5 mm thickness cannot withstand the load due to low factor of safety (0.447), while angular mild steel (10 mm) showed a good factor of safety of (1.79), which is highly adequate to support the plant's chamber. Therefore, any angular mild steel of diameter ranging 5 mm -10 mm would be adequate. All other designed parameters (stress, strain, deflection, and thermal resistance) were within the acceptable standard, this portrayed design adequacy.

vii. Simulation analyses outcomes of the components of the micro steam power plant were in agreement to that of conventional design.

viii. Designed temperature of 0- 400^{o}C was clearly within the acceptable range and far from maximum tolerable temperature of 1200^{o}C.

ix. There are more heating effects inside the chamber and the heat loss is negligible. This shows that the material can withstand the thermal effect even beyond 1200^{o}C. Hence, the furnace chamber can operate normally under temperature higher than of 400 ^{o}C.

x. Ability of the system to superheat from 450 to 1400.2 ^{o}C based on the simulation results is an indication that the maximum designed superheated temperature of 400- 450 ^{o}C could be accommodated.

xi. Heat flux (2.31 W/mm^2) obtained from the design was conveniently within the range, which shows that the design is workable.

xii. Locally sourcing of many materials and equipment used to develop the plant is an indication of sustainability.

REFERENCES

1. Adeline, Rand Juan, A. (2012): Numerical Characterization of the aerodynamic in fixed grate biomass burners. Computer and Fluid, Vol. 45-53.
2. Adewumi I. K. and M. O. Ogedengbe (2025): Optimizing Conditions for Activated Charcoal Production from Palm Kernel Shells.J of Applied Sciences. Vol. 5, 2005 pp 1082-1087
3. Aho, M. (2001): Reduction of chlorine deposition in FB boiler with aluminum containing additives. Fuel, 880, pp. 1943-1951
4. Ajayi, A (2007): Nigeria energy challenge and power development: The way forward, Bulletin of Science Association of Nigeria Vol 28. Pp 1-3
5. Astrom, K.J. and Bell, R.D. (2000): Drum-boiler dynamic Automatica Vol.36, pp.363-378
6. Awosope, C. O. and Okoye, C. U. (2003): "Rural Electrification: Emerging Technical Considerations for Sustainability in a Developing Economy" , Proceeding of the Nineteenth Annual National Conference of Nigerian society of Engineers (Electrical Division), Lagos. Oct 2-3, pp 25-30
7. Binstock, D. Yeager, P. and Grohse, G. (1989):.Validation of a method for determining element in solid waste.
8. Ekpo. E. (2005): 'Hydro potential and Development plans in Nigeria. Hydropower and Dams Journal, Volume twelve, Issue 6, pp 58-62.

9. Ekpo. E. (2012): ' Hydropotential and Development plans in Nigeria" The Water Engineer Newsletter of the Water Division of the Nigerian Society of Engineers December 2012, Vol 1, Issue 2, pp 5-9.
10. Elefe S. K., Kareem B., Ayodeji O. (2024). Performance Enhancement of a Failed Steam Generator, International Journal of Research and Innovation in Applied Science (IJRIAS), IX(VIII), DOI: 10.51584/IJRIAS
11. Husain, Z., Z. Zaine and Z. Abdullah, (2002). Briquetting of Palm fibre and shell from processing of palm nuts to palm oil. Biomass Bio-energy Vol. 22, pp 505 – 509
12. Izar, S.O. Ohimain, E and Angaye, T. (2016): Potential Thermal Energy from Palm Oil processing Solid wastes in Nigeri: mills Consumption and Surplus Quantification. BritishJournal of renewable Energy, 01(01), 39-45
13. Jekayinfa, S.O. and Bamgboye,A. I.(2008): Energy use analysis of selected palm- kernel oil mills in south western Nigeria. Energy, Vol. 33, pp. 81-90
14. Joller, M., Brunner T., Obernberger, I., (2007): Modelling of Aerosol Formation during Biomass Combustion for Various Furnace Type. FuelProcessingTechnol, Vol.88, 1136-47. Journal of physics, series 1007, pp.1-6.
15. Kareem B. and Babatunde D. D. (2018). Optimization of Energy Content of Palm Kernel Shell (PKS) Using Modelling Approach, International Journal of Advance Industrial Engineering, 6, 111-117.
16. Kareem B., Ewetumo T., Adeyeri M. K. and Oyetunji A. (2018a). Design of Steam Turbine for Electric Power Production using Heat Energy from Palm Kernel Shell, Journal of Power and Energy Engineering, 06(11), 111-125.
17. Kareem B., Ewetumo T., Adeyeri M. K., Oyetunji A., Olowookere S. T. (2018b). Development of Electricity Generating System for a Micro Power Plant, Journal of production engineering, 21(2), 43-50.
18. Kareem B., Oladosu K. O., Alade A. O., Durowoju M. O. (2018c). Optimization of Combustion Characteristics of Palm-Kernel Based Biofuel for Grate Furnace, International Journal of Energy and Environmental Engineering, 9, 457-472.
19. Khullar, C. (1995): The use of “combustion additives” to improve heat transfer and reduce combustion emissions in package boilers. In proceedings of the second international conference on combustion and emission control. London, UK: Institute of Energy pp.168-77
20. Makoju,1. O. (2003) "Quantifying the Electricity Supply Gap A Simplistic Treatment" Proceeding of the Nineteenth Annual National Conference of Nigerian Society of Engineers (Electrical Division), Lagos. Oct 2-3, pp 1-
21. Marrow, (2005): Renewable fuel grate firing combustion technology- The European Experience. Available from http://www.gov/doer/rps/mor_rpt.pdf. (Accessed 10 June, 2014)
22. MNNA, (2001): Long term benefit oil palm biomass. Be Malaysian National News Agency Press Release.
23. Mohammed, A., Tjahjono, H and Metal, R. (2014): Analysis of Palm Biomass as Electricity from Palm Oil Mills in North Sumatera. Energy procedia, 47, pp. 166-172
24. Najmi, W.M., Rosil, A.N. and Izat, M., S (2007): Combustion Characteristics of Palm Kernel shells using an inclined Grate Combustor. Journal of Faculty of Mechanical Engineering, UiTM, Malaysia, pp. 15-28
25. Okpula D. C. (1990): Palm Kernel Shell as a lightweight aggregate in concrete. Building and Environment, Vol. 25, number 4, 1990, pp 291 -296
26. Oladosu K. O. (2016) Optimization of Combustion of Palm Kernel shell, in a Grate Furnace for Superheated Steam Generation. Ph.D Thesis, Mechanical Engineering Department, Federal University of Technology Akure, Nigeria
27. Oladosu, K, O. Kareem, B. Akinnuli, B.O. and Asafa, T. B. (2016) Optimization of Ash Yield from Combustion of palm kernel and Selected Additives (Al_2O_3, CaO and MgO) Using D-Optimal Design. Leonard Electronic Journal of Practices and Technologies, No28, 9-18
28. Oladosu., K. O. Kareem., B. Akinnuli, B. O. and Asafa, T. B. (2017) Application of Computer Aided Design of a Scalable Combustion Furnace Using Palm Kernel Shell as Heat Source . Acta Technical Corviniensis-Bulletin of Engineering, I, 127-134

29. Oladosu., K. O., Ajayeoba, A. O. Kareem B and Akinnuli, B.O. (2018) Development and Cost Estimation for Sizing 5KW Palm Kernel shell steam Boiler. American Journal of Engineering Research (AJER), 7, 113-122
30. Pettersson, L. and Steenari, B. (2009): Chemical fractioning for the characterization of fly ash from combustion of biofuels using different methods of alkali reduction. Fuel, Vol. 88 pp 1758-1772.
31. Pichet, N. and Vladimir I. (2014): Combustion of palm kernel shell in a fluidized bed: Optimization of biomass particle size and operating conditions. Energyconversion and management,pp.1-9. http://dx.doi.org/10.1016/j.enconman.2014.01.054.
32. Sebastian, T. (2002): Thermal Design of Heat Exchangers. Energy Engineering and Environmental Protection, pp. 4-9.
33. Sjaak, V. and Jaap, K. (2008): Handbook of biomass combustion and co-firing, ISBN-13:978-1849711043.
34. Sumanttin, S. and Chai, S. M. (2008): Utilization of oil palm as a source of renewable "energy in Malaysia. Renewable sustainable Energy, Vo1.l2, No 9 pp.04-21.
35. Thomas, R., Jabouille, F. and Torero, J. L (2009): Effect of excess air on grate combustion of solid wastes and on gaseous products. International Journal of thermal Sciences. Pp 165-173
36. Yin, C. Rosendahl,L and Kar S.K. (2008): Grate-firing of biomass for heat and power production. Progress in Energy and combustion Science, Vol. 34, pp. 725-754
37. Yusniati, (2018): Biomass analysis at palm oil factory as an electric power plant.